Frequency-Domain Analysis of Control Loops With Intermittent Data Losses

Duarte Antunes and W. P. M. H. Heemels

Abstract—In this technical note, we propose a frequency-domain analysis framework for control systems with data losses, assumed to be statistically independent over time. Based on our framework, the amplitudes of the mean and variance of the output response to a sinusoidal input can be plotted as a function of the input frequency, much like in the classical Bode plot. Analogously to the classical analysis, this plot can be used for inferring the behavior of the output response, characterized now by its mean and variance, to an arbitrary input signal.

Index Terms—Data loss, frequency response methods, packet drops, stochastic analysis.

I. Introduction

In several contexts, a real-time control loop is intermittently disrupted by undesired events causing imperfect control updates. These events include packet drops in wireless communication, task deadline misses in shared processors, and outliers in sensor data, and can often be modeled as data losses.

A common solution to cope with such losses is to use the most recently received data as an estimate of the missing data. This solution can be captured by a *time-varying* model and various methods are available in the literature to analyze such models (see, e.g., [1]–[3]). However, the majority of these methods rely on time-domain analysis. Frequency-domain analysis is typically not an option in this context since it is restricted to *time-invariant* systems (cf. [4]). As a result, for a control loop with data losses it is not straightforward to reason about the behavior of output responses to arbitrary input signals, which for time-invariant systems is enabled by frequency response (Bode) plots. One of the few works using frequency-domain ideas is [1], in which the analysis is based on the power spectral density of the output response to white noise. While this approach is useful to assert the impact of stochastic disturbance inputs, it is not clear how to infer the output response to deterministic inputs (e.g. reference signals).

Motivated by the relevance of frequency-domain analysis in engineering practice, in this technical note we develop a frequency-domain analysis framework for a time-varying model capturing lossy closed loops in which the data losses are statistically independent over time. Note that this is a reasonable assumption in many of the aforementioned contexts. Key to our approach is the observation that the maps between the input of the loop and the statistical moments of the state and of the output are *time-invariant*. Using this observation, we show that the amplitudes of the mean and variance of the output response to sinusoidal input signals can be plotted as a function of the input
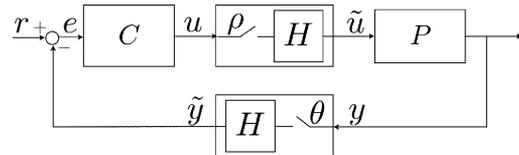
Fig. 1. Setup; P-plant, C-controller, $\rho_t \in \{0, 1\}$, and $\theta_t \in \{0, 1\}$ determine if data losses occur at time $t \in \mathbb{Z}$; H represents the hold scheme (3), (4), by which the most recently received data is hold constant in case of a data loss.

frequency, similarly to the classical frequency response (Bode) plot. Moreover, analogously to the classical analysis, this plot allows for inferring the behavior of the output response, characterized now by its mean and variance, to an arbitrary deterministic input. Interestingly, the output mean can be *exactly* computed by a procedure which involves replacing the lossy data links by first-order linear systems while the ouput variance can be *upper bounded* by a graphical method. By combining these results one can assert the influence of the bandwidth of the input signal and of the data loss probabilities on the mean and variance of the output response.

The technical note is organized as follows. Section II formulates the problem, Section III presents the main results, and Section IV provides an example. The focus is on a single-input single-output system with data losses modeled as hold operators. Section V provides concluding remarks, briefly discussing how to extend the ideas to other cases of interest.

II. Problem Formulation

Consider the feedback loop depicted in Fig. 1, where data losses can occur in the links from the sensor to the controller and from the controller to the actuator. The plant and the controller are assumed to be described by the linear models

$$x_{t+1} = Ax_t + B\tilde{u}_t, \quad y_t = Cx_t \tag{1}$$

$$x^c_{t+1} = A_c x^c_t + B_c(r_t - \tilde{y}_t), \quad u_t = C_c x^c_t + D_c(r_t - \tilde{y}_t) \tag{2}$$

respectively, where $x_t \in \mathbb{R}^{n_x}$ and $x^c_t \in \mathbb{R}^{n_v}$ denote the state of the plant and of the controller at time $t \in \mathbb{Z}$, respectively. Moreover, $\tilde{u}_t \in \mathbb{R}$ and $y_t \in \mathbb{R}$ are the input and the output of the plant at time t, respectively. Similarly, $e_t := r_t - \tilde{y}_t$ and $u_t \in \mathbb{R}$ are the input and the output of the controller at time t, respectively, where $\tilde{y}_t \in \mathbb{R}$ is the latest received output of the plant and $r_t \in \mathbb{R}$ is the reference signal.

To cope with data drops in the link between the sensor and the controller, we assume that the controller updates $\tilde{y}_t$ as a function of y_t according to the following hold scheme:

$$\tilde{y}_t = (1 - \theta_t)\tilde{y}_{t-1} + \theta_t y_t \tag{3}$$

for $t \in \mathbb{Z}$, where θ_t equals one if the controller receives the output of the plant at time t and zero if this data is lost. Similarly, to cope with data drops in the link between the controller and the actuator of the plant, we assume that the actuator updates the control input to the plant according to

$$\tilde{u}_t = (1 - \rho_t)\tilde{u}_{t-1} + \rho_t u_t \tag{4}$$

for $t \in \mathbb{Z}$, where ρ_t equals one if the actuator receives the output of the controller at time t and zero otherwise. Note that the implementation of this scheme is straightforward. In fact, the controller runs (2), (3) based on the received output measurements $\{y_t | \theta_t = 1\}$ and outputs the control input u_t at every time t; the actuator runs (4) based on the controller output $\{u_t | \rho_t = 1\}$ and outputs the actuation values $\tilde{u}_t$ at every time t.

Let $\sigma_t \in \{1, 2, 3, 4\}$ indicate which of the following data loss possibilities occurred at time t:

$$(\theta_t, \rho_t) = \begin{cases} (0,0) & \text{if } \sigma_t = 1 \\ (1,0) & \text{if } \sigma_t = 2 \\ (0,1) & \text{if } \sigma_t = 3 \\ (1,1) & \text{if } \sigma_t = 4. \end{cases}$$

Then, if we let $\xi_t := (x_t, x_t^c, \tilde{u}_{t-1}, \tilde{y}_{t-1})$, we can write

$$\xi_{t+1} = E_{\sigma_t} \xi_t + H_{\sigma_t} r_t \qquad (5)$$

for every $t \in \mathbb{Z}$, where E_i, for $i \in \{1, 2, 3, 4\}$ is shown at the bottom of the page. Note that $(\theta_t, \rho_t) = (\underline{\theta}_{\sigma_t}, \underline{\rho}_{\sigma_t})$. Moreover,

$$y_t = F \xi_t, \quad F := (C \quad 0 \quad 0 \quad 0). \qquad (6)$$

The model is now completed by assigning probabilities to the occurrence of the data loss possibilities for which we adopt the following assumption.

Assumption 1: For every $t_1 \in \mathbb{Z}$, $t_2 \in \mathbb{Z}$, $t_1 \neq t_2$, σ_{t_1} and σ_{t_2} are independent and identically distributed.

Under this assumption, the following probabilities do not depend on time:

$$p_i := \text{Prob}[\sigma_t = i], \quad q_\theta := \text{Prob}[\theta_t = 1], \quad q_\rho := \text{Prob}[\rho_t = 1]$$

for every $t \in \mathbb{Z}$, $i \in \{1, 2, 3, 4\}$.

Model (5) together with the probabilities p_i, $i \in \{1, 2, 3, 4\}$, forms a special case of a Markov jump linear system [5]. This model can capture different scenarios of interest. For example, the case in which the controller and sensors use a shared communication medium and thus cannot transmit at the same time can be described by $\text{Prob}[\sigma_t = 4] = 0$. Another example is the case where they use two different transmission channels. This includes the case where only one of the channels is lossy, which can be captured by either $\text{Prob}[\sigma_t \in \{1, 2\}] = 0$ or $\text{Prob}[\sigma_t \in \{1, 3\}] = 0$.

While we are interested in the forced response of (5) to the input r, we can consider the unforced response ($r_t = 0$, for all $t \in \mathbb{Z}$) for a given initial condition ξ_0. We assume the following stability notion, typically considered for unforced Markov jump linear systems (see [5]).

Assumption 2: We assume that the (unforced) system (5) with $r_t = 0$, for all $t \in \mathbb{Z}$, is mean square stable, i.e., for every ξ_0, $\lim_{t \to \infty} \mathbb{E}[\|\xi_t\|^2] = 0$.

A necessary and sufficient condition to test mean square stability is given below [see (19)]. Note that if the (unforced) system (5) is mean square stable then $\xi_t \to 0$ as $t \to \infty$ with probability one (see [5, Cor. 3.46]).

The problem addressed in this technical note is the computation of the statistical moments of the output responses of the closed-loop system (5) to a deterministic input r. We denote by $\hat{r}(z) := \sum_{t=-\infty}^{\infty} r_t z^{-t}$ the z-transform of r and assume that r either belongs to the class of signals with bounded energy, i.e., $\sum_{t=-\infty}^{\infty} |r_t|^2 < \infty$, or to the class of periodic bounded signals (power signals). While in the former case the Fourier transform $\hat{r}(e^{j\omega})$ exists for $\omega \in [0, 2\pi)$ [6], in the latter case $\hat{r}(e^{j\omega})$ is a generalized function described by

$$\hat{r}(e^{j\omega}) = \frac{2\pi}{T} \sum_{k=0}^{T-1} v_k \delta \left(\omega - \frac{2\pi k}{T} \right), \quad \omega \in [0, 2\pi) \qquad (7)$$

where T denotes the period, $v_k := \sum_{t=0}^{T-1} r_t e^{-j(2\pi k/T)t}$, and δ denotes the Dirac function [6]. A special case of a deterministic input is the sinusoid

$$r_t = \Im\{v e^{j\omega_c t}\} = |v| \sin(\omega_c t + \psi_v) \qquad (8)$$

where $v = |v| e^{j\psi_v} \in \mathbb{C}$ is the complex amplitude, $\omega_c \in [0, 2\pi)$ is the frequency, and $\Im$ denotes the imaginary part.

While we focus on the output y, we could also consider other outputs such as the tracking errors $y - r$ or $\tilde{y} - r$.

III. FREQUENCY-DOMAIN ANALYSIS

In Sections III-A and B, we discuss how to compute the first and second moments of the output response, respectively. Based on these results, in Section III-C we define a frequency response plot and discuss how this plot allows for reasoning about the behavior of the output response.

A. Expected Value

Although (5) is time-varying, the behavior of the expected values, under Assumption 1, is governed by a linear time-invariant system as we show next.

Theorem 1: Suppose that Assumptions 1 and 2 hold. Then

$$\beta_{t+1} = \bar{E} \beta_t + \bar{H} r_t, \quad \beta_t := \mathbb{E}[\xi_t], \ t \in \mathbb{Z} \qquad (9)$$

where $\bar{H} := \sum_{i=1}^{4} p_i H_i$, $\bar{E} := \sum_{i=1}^{4} p_i E_i$, and the eigenvalues of $\bar{E}$ lie inside the open unit circle. In particular, the z-transform of the expected value of the output $\hat{y}(z) := \sum_{t=-\infty}^{\infty} \mathbb{E}[y_t] z^{-t}$ is given by

$$\hat{y}(z) = a(z) \hat{r}(z) \qquad (10)$$

for z in the intersection of the regions of convergence of $\hat{r}(z)$ and $a(z)$, where $a(z) := F(zI - \bar{E})^{-1} \bar{H}$. Moreover, if r_t is a sinusoid (8), then

$$E_i := \begin{pmatrix} A - \underline{\rho}_i \underline{\theta}_i BD_c C & \underline{\rho}_i BC_c & (1 - \underline{\rho}_i)B & -\underline{\rho}_i(1 - \underline{\theta}_i)BD_c \\ -\underline{\theta}_i B_c C & A_c & 0 & -(1 - \underline{\theta}_i)B_c \\ -\underline{\rho}_i \underline{\theta}_i D_c C & \underline{\rho}_i C_c & (1 - \underline{\rho}_i) & -\underline{\rho}_i(1 - \underline{\theta}_i)D_c \\ \underline{\theta}_i C & 0 & 0 & (1 - \underline{\theta}_i) \end{pmatrix}$$

$$H_i := \left(\underline{\rho}_i (BD_c)^\top \quad B_c^\top \quad \underline{\rho}_i D_c^\top \quad 0 \right)^\top$$

$$(\underline{\theta}_1, \underline{\rho}_1) := (0, 0), (\underline{\theta}_2, \underline{\rho}_2) := (1, 0)$$

$$(\underline{\theta}_3, \underline{\rho}_3) := (0, 1), (\underline{\theta}_4, \underline{\rho}_4) := (1, 1).$$

$\mathbb{E}[y_t]$ is a sinusoid described by

$$\mathbb{E}[y_t] = \Im \left\{ a(e^{j\omega_c})v e^{j\omega_c t} \right\}. \tag{11}$$

Proof: Taking expected values on both sides of (5), we obtain

$$\mathbb{E}[\xi_{t+1}] = \mathbb{E}\left[E_{\sigma_t} \xi_t \right] + \mathbb{E}\left[H_{\sigma_t} \right] r_t. \tag{12}$$

From (5), we conclude that ξ_t depends only on σ_s for $s < t$. Thus, ξ_t is statistically independent of σ_t under Assumption 1 for each $t \in \mathbb{Z}$. Then, $\mathbb{E}[E_{\sigma_t}\xi_t] = \mathbb{E}[E_{\sigma_t}]\mathbb{E}[\xi_t] = \bar{E}\beta_t$, and (9) holds. Moreover, Assumption 2 assures that (9) is a stable system in the sense that β_t converges to zero as $t \to \infty$ for every initial β_0, when the input r is identically zero (or equivalently the eigenvalues of $\bar{E}$ lie inside the open unit circle). This follows from the fact that $\mathbb{E}[\xi_{i,t}]^2 \leq \mathbb{E}[\xi_{i,t}^2]$ for every component $\xi_{i,t}$ of ξ_t. Using standard arguments for linear time-invariant systems (see, e.g., [4, Ch. 8] and [6, Ch. 10]), we can relate the z-transforms of the input $\hat{r}(z)$ and of the expected value of the output by (10), and conclude that (11) is the output response $\mathbb{E}[y_t] = F\beta_t$ of (9) to (8). ∎

Note that $\mathcal{R} := \{z \in \mathbb{C} \mid |z| > 1\}$ is included in the region of convergence of $\hat{r}(z)$ for the aforementioned input signals of interest. Moreover, since $a(z)$ is a rational function of z with roots coinciding with the eigenvalues of $\bar{E}$, its region of convergence includes $\{z \in \mathbb{C} \mid |z| > \bar{\lambda}\}$, where $\bar{\lambda}$ denotes the largest absolute value of the eigenvalues of $\bar{E}$ (see [6, Ch. 10]), which must be smaller than 1 due to Theorem 1. Thus, $\mathcal{R}$ is also in the region of convergence of $a(z)$.

The next proposition provides a simple way of computing $a(z)$ when θ_t and ρ_t are independent. For $d \in [0, 1]$, let

$$f_d(z) := \frac{d}{1 - (1 - d)z^{-1}}.$$

Proposition 1: Suppose that Assumption 1 holds and that θ_t and ρ_t are independent random variables for each $t \in \mathbb{Z}$. Then

$$a(z) = \frac{\tilde{p}(z)}{1 + p(z)} \tag{13}$$

where $p(z) = f_{q_\theta}(z)\tilde{p}(z)$ and

$$\tilde{p}(z) := C(zI - A)^{-1}B f_{q_\rho}(z) \left(C_c(zI - A_c)^{-1}B_c + D_c \right).$$

Proof: If θ_t and ρ_t are independent for each $t \in \mathbb{Z}$, then we get the equation (14), shown at the bottom of the page.

Then (13) is obtained by computing the transfer function (10) from r to $\mathbb{E}[y]$ using (14). ∎

One can observe that (9), with matrices as in (14), describes a linear time-invariant closed-loop system in which the lossy links associated with θ_t and ρ_t are replaced by first-order systems given by $f_{q_\theta}(z)$ and $f_{q_\rho}(z)$, respectively. We can then use this result to compute expected values of other output responses. For example, we can obtain $\hat{e}(z) = (1/(1 + p(z)))\hat{r}(z)$, where $\hat{e}(z) := \sum_{t=-\infty}^{\infty} \mathbb{E}[e_t]z^{-t}$. Note the resemblance of this expression and of (10) and (13) with similar expressions in the context of frequency-domain analysis for linear time-invariant systems [4], which are recovered when there are no data losses ($q_\rho = q_\theta = 1$). For example, $\hat{e}(z)$ is related to $\hat{r}(z)$ by a function which plays the role of a sensitivity function.

B. Variance

The variance of the output is given by

$$\text{var}(y_t) := \mathbb{E}\left[(y_t - \mathbb{E}[y_t])^2 \right] = \mathbb{E}\left[y_t^2 \right] - \mathbb{E}[y_t]^2. \tag{15}$$

The second term in this expression can be obtained by squaring the inverse z-transform of (10). To compute the first term, we start by noticing that

$$\mathbb{E}\left[y_t^2 \right] = G\zeta_t \tag{16}$$

where $G := F \otimes F$, $\otimes$ denotes the Kronecker product, $\zeta_t := \mathbb{E}[\xi_t \otimes \xi_t]$, and we used the fact that

$$(A \otimes B)(C \otimes D) = (AC) \otimes (BD) \tag{17}$$

for matrices with compatible dimensions. From (5), we obtain

$$\zeta_{t+1} = M\zeta_t + L\beta_t r_t + N r_t^2 \tag{18}$$

where

$$M := \sum_{i=1}^{4} p_i E_i \otimes E_i, \ N := \sum_{i=1}^{4} p_i H_i \otimes H_i$$

$$L := \sum_{i=1}^{4} p_i (E_i \otimes H_i + H_i \otimes E_i)$$

and we used again (17) and similar arguments as the ones used in the proof of Theorem 1 under Assumption 1. One can show that Assumption 2 is equivalent to

$$\mathrm{r}(M) < 1 \tag{19}$$

where r denotes the spectral radius (see [5]).

Contrarily to the equation describing the first moment (9), the system (18) depends non-linearly on the input r_t, $t \in \mathbb{Z}$. Yet, as we show next, we can (i) exactly characterize the solution to (18), and thus compute (15), when r is a sinusoidal input, described by (8); and (ii) use this fact to provide a bound for the variance (15) to an arbitrary input signal characterized by its Fourier transform $\hat{r}(e^{j\omega})$, $\omega \in [0, 2\pi)$.

Theorem 2: Suppose that Assumptions 1 and 2 hold and let y be the output response (6) of (5) to the input (8). Then

$$\text{var}(y_t) = b(e^{j\omega_c})|v|^2 - \Re\left\{ c(e^{j\omega_c})v^2 e^{2j\omega_c t} \right\} \tag{20}$$

for every $t \in \mathbb{Z}$, where, for $z \in \mathbb{C}$

$$b(z) := \frac{1}{2}\Re\left\{ G(I - M)^{-1}\left(N + L(zI - \bar{E})^{-1}\bar{H} \right) \right\} - \frac{|a(z)|^2}{2}$$

$$c(z) := \frac{1}{2}G(z^2 I - M)^{-1}\left(N + L(zI - \bar{E})^{-1}\bar{H} \right) - \frac{a(z)^2}{2}$$

and $\Re$ denotes the real part. Moreover, $b(1) = c(1) = 0$ and $b(-1) = c(-1)$, and thus $\text{var}(y_t) = 0$ for every $t \in \mathbb{Z}$ when $\omega_c = 0$ and when $\omega_c = \pi$.

$$\bar{E} = \begin{pmatrix} A - q_\rho q_\theta B D_c C & q_\rho B C_c & (1 - q_\rho)B & -q_\rho(1 - q_\theta)B D_c \\ -q_\theta B_c C & A_c & 0 & -(1 - q_\theta)B_c \\ -q_\rho q_\theta D_c C & q_\rho C_c & (1 - q_\rho) & -q_\rho(1 - q_\theta)D_c \\ q_\theta C & 0 & 0 & (1 - q_\theta) \end{pmatrix}$$

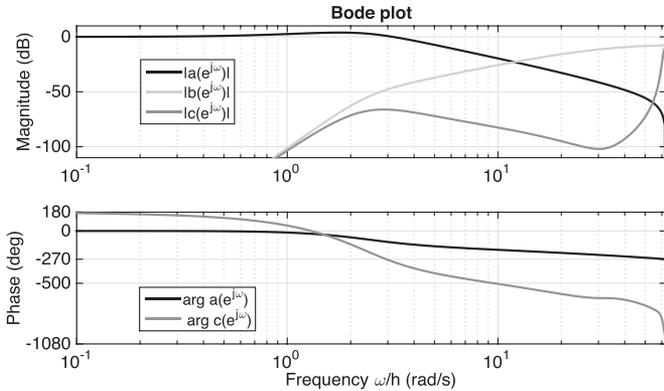$$\bar{H} = \begin{pmatrix} q_\rho(B D_c)^\top & B_c^\top & q_\rho D_c^\top & 0 \end{pmatrix}^\top \tag{14}$$

Fig. 2.   Frequency response of mean and variance, $q_\rho = 0.8$.

Theorem 3: Suppose that Assumptions 1 and 2 hold and let y be the output response (6) of (5) to a reference input r with Fourier transform $\hat{r}(e^{j\omega})$, $\omega \in [0, 2\pi)$. Then, for r with bounded energy, it holds that

$$\text{var}(y_t) \leq \frac{2}{\pi} \int_0^\pi \left(\left| b(e^{j\omega}) \right| + \left| c(e^{j\omega}) \right| \right) \left| \hat{r}(e^{j\omega}) \right|^2 d\omega \qquad (21)$$

for every $t \in \mathbb{Z}$. Moreover, for T-periodic r with Fourier transform (7), it holds that

$$\text{var}(y_t) \leq \frac{4}{T} \sum_{k=1}^{\lfloor \frac{T}{2} \rfloor} \left(\left| b(e^{j\omega_k}) \right| + \left| c(e^{j\omega_k}) \right| \right) |v_k|^2 \qquad (22)$$

for every $t \in \mathbb{Z}$, where $\omega_k := 2\pi k/T$, the values v_k are described after (7), and $\lfloor T/2 \rfloor = (T/2) - 1$ if T is even and $\lfloor T/2 \rfloor = (T-1)/2$ if T is odd.

Note that (21) provides a constant bound for every time $t \in \mathbb{N}$. In the proof of Theorem 3, given in the Appendix, we obtain stricter bounds, which depend on t (see Remark 4).

C. Reasoning in Terms of Frequency Response Plots

We propose to characterize the map between the input and the mean and the variance of the output by: (i) a magnitude plot, which consists of the following three graphs $(\omega, |a(e^{j\omega})|)$, $(\omega, |b(e^{j\omega})|)$, $(\omega, |c(e^{j\omega})|)$ $\omega \in [0, \pi]$ and (ii) a phase plot, which consists of the following two graphs $(\omega, \arg(a(e^{j\omega})))$, $(\omega, \arg(c(e^{j\omega})))$, $\omega \in [0, \pi]$, where $\arg(a)$ denotes the argument of $a \in \mathbb{C}$. Log-scales may be used for convenience (see Fig. 2). Then, the following procedure allows to obtain insights on the mean and the variance of the output response to a reference r with bounded energy.

1) Multiply $a(e^{j\omega})$ and $\hat{r}(e^{j\omega})$ and obtain the expected value of the output by inverting the Fourier transform $a(e^{j\omega})\hat{r}(e^{j\omega})$, $\omega \in [0, 2\pi)$.
2) Multiply $|\hat{r}(e^{j\omega})|^2$ by $|b(e^{j\omega})| + |c(e^{j\omega})|$, for $\omega \in [0, \pi]$, and obtain a bound for the variance at every time step $t \in \mathbb{Z}$ by computing (21). Graphically (see Fig. 4), the computation of (21) amounts to plotting $(|b(e^{j\omega})| + |c(e^{j\omega})|)|\hat{r}(j\omega)|^2$, for $\omega \in [0, \pi]$, and computing the average over frequency multiplied by a factor 2.

The computation of the expected value is very close to the procedure to compute the output response in the context of linear time-invariant systems [4], which is a special case when there are no data losses ($q_\theta = q_\rho = 1$). As for the variance, from Theorem 2 we know that the plots of $b(e^{j\omega})$ and $c(e^{j\omega})$ are equal to zero for $\omega = 0$. By continuity, $b(e^{j\omega})$ and $c(e^{j\omega})$ are also close to zero for low frequencies. If we consider
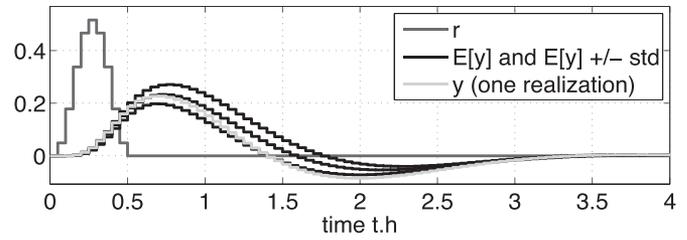

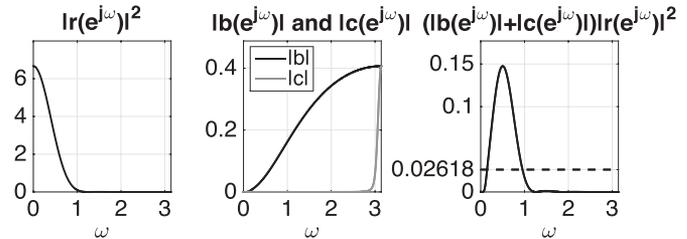Fig. 3.   Time-responses for $T_r = 10$, $q_\rho = 0.8$.

Fig. 4.   Computation of the bound for the variance.

a bandwidth limited input signal, then $(|b(e^{j\omega})| + |c(e^{j\omega})|)|\hat{r}(j\omega)|^2$ will be approximately zero for very low and very high frequencies (close to $\omega = \pi$) and thus be concentrated in a given range of intermediate frequencies. Hence, increasing the bandwidth of the input signal will in general lead to an increase in the variance of the output response, the extent to which can be bounded by (21). Moreover, for a desired frequency range for the input signal plotting $b(e^{j\omega})$ and $c(e^{j\omega})$ for different values of the data loss probabilities one can infer how the variance of the output response varies with these probabilities. Note that for $q_\theta = 1$ and $q_\rho = 1$, $b(e^{j\omega})$ and $c(e^{j\omega})$ are zero for every $\omega \in [0, \pi]$.

From the expected value and the variance one can infer the behavior of the sample paths of the output. In fact, from Chebychev's inequality, we conclude that, for $\alpha < 1$

$$\text{Prob}\left[|y_t - \mathbb{E}[y_t]| > \alpha \, \text{std}(y_t) \right] \leq \frac{1}{\alpha^2}, \quad t \in \mathbb{Z} \qquad (23)$$

where $\text{std}(y_t) := \sqrt{\text{var}(y_t)}$ denotes the standard deviation. One can then use the bound (21) to provide a guarantee on the probability that the output response is not far from its expected value.

IV. EXAMPLE

Let the plant be a double integrator described by the transfer function $1/s^2$ and the controller be described by the transfer function $10(s + 1)/(s + 5)$. The plant and the controller are discretized at a sampling period $h = 0.05$ with the zero-order hold invariant method [4] leading to the matrices in (1) and (2). We consider that $q_\rho = 0.8$ and $q_\theta = 1$, i.e., in the setup of Fig. 1 data losses occur only in the link between the controller and the plant. We consider the following class of reference inputs r defined in terms of the Hann function:

$$r_t = \begin{cases} \gamma \frac{1}{2} \left(1 - \cos\left(\frac{2\pi t}{T_r} \right) \right), & t \in \{0, 1 \ldots, T_r\} \\ 0, & \text{otherwise} \end{cases} \qquad (24)$$

where γ is a normalization factor such that r has unitary energy, i.e., $\sum_{t=-\infty}^{\infty} r_t^2 = 1$.

Fig. 2 plots the frequency response of the mean and the variance proposed in Section III-C. Fig. 3 plots the input for $T_r = 10$, a realization of the output, and the expected value of the output. It also plots two signals obtained by adding and subtracting the standard deviation to the expected value. This is convenient since from Chebychev's
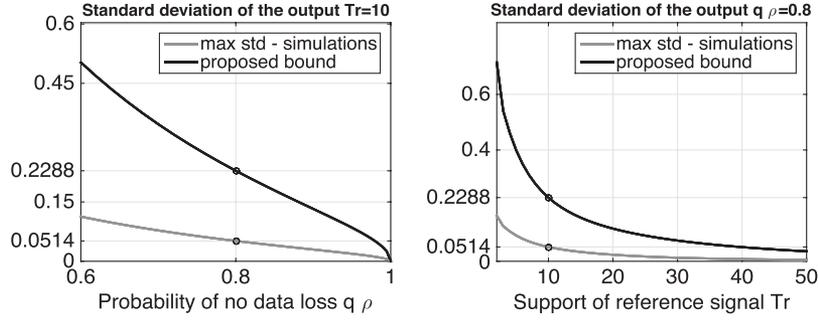
Fig. 5. Output variance as a function of T_r and q_ρ.

inequality (23), one can guarantee that the realizations at a given time $t \in \mathbb{Z}$ lie in between these plotted offsets with respect to the expected value multiplied by a factor α with probability larger than $1/\alpha^2$. The mean is obtained by running (9) for the input (24). The standard deviation is obtained by running (18) for the input (24) and taking the square root of (20). The obtained maximum standard deviation is given by 0.0514.

The bound for the variance obtained from (21) is given by 0.05236 which corresponds to a standard deviation of 0.2288. Note that this bound is within a factor 5 from the maximum value of the actual standard deviation 0.0514. The computation of this bound is illustrated in Fig. 4, considering linear scales. As mentioned in Section III-C we start by computing $|\hat{r}(e^{j\omega})|^2$ and multiplying by $|b(j\omega)| + |c(j\omega)|$. The variance bound is obtained by computing the average value over frequency and multiplying by 2.

On the right side of Fig. 5, we plot the maximum values of the standard deviation of the output response to (24) and the bound (21) as a function of the drop probability for $T_r = 10$. On the left, the same plots are shown as a function of T_r for a no loss probability $q_\rho = 0.8$. Increasing the bandwidth of the input signal (decreasing T_r) and increasing the drop probability leads to a larger variance as expected from the remarks in Section III-C. We conclude again that the bounds are reasonably close to the values obtained by simulation.

V. DISCUSSION

In this work, we have shown that the maps between an input of a closed-loop system with data losses and the statistical moments of the state and output are described by time-invariant models, provided that the losses are independent and identically distributed. Building upon this fact, we proposed an analysis using the output mean and variance frequency response, with similar features to the classical analysis for time-invariant systems and similar advantages when compared to a time-domain analysis. In fact, while a time-domain analysis allows only to infer the behavior of the output response to a *single* input by plotting (several) output realizations or the statistical moments, a frequency-domain analysis provides a magnitude and phase plot, invariant with respect to the input. As a result, such plots allows to reason on the behavior of the output response to an *arbitrary* input.

The main ideas presented in this work can be extended to analyze scenarios which can still be modeled by (5) for different dynamic and input injection matrices. Such model can capture multiple-input multiple-output (MIMO) linear plants, other deterministic inputs such as a plant disturbance, or sensor noise, and other time-varying artifacts in the control loop such as delays with arbitrary distributions. One can also show that a different mechanism for handling data losses by which $\tilde{y}_t$ and $\tilde{u}_t$ are set to zero if data loss occurs in the associated link at time t can be modeled by (5) and the proposed framework can be applied (see [7]).

While we have opted to restrict our analysis to the first two moments, an analysis using higher-order moments can be pursued. In fact, similarly to (18) we can write $\zeta_{t+1}^n := \mathbb{E}[\underbrace{x_{t+1} \otimes x_{t+1} \otimes \ldots \otimes x_{t+1}}_{n}]$, in terms of the products $\zeta_t^m r_t^{n-m}$ for $m \in \{0, 1, \ldots, n\}$. As in (16), we can write the output statistical moment $\mathbb{E}[y_t^n]$ in terms of ζ_t^n and exactly characterize their input response to a sinusoidal input.

APPENDIX
PROOF OF THEOREM 2

Under Assumptions 1 and 2, we conclude from Theorem 1 that the expected value of the state response β to (8) is a vector of sinusoids with frequency ω_c and complex amplitudes $w(e^{j\omega_c})v$, $w(z) := (zI - \bar{E})^{-1}\bar{H}$ [cf. (9)], and $\mathbb{E}[y_t]$ is a sinusoid with frequency ω_c and complex amplitude $a(e^{j\omega_c})v$. Thus

$$\mathbb{E}[y_t]^2 = \frac{1}{2}\left(\left|a(e^{j\omega_c})\right|^2 |v|^2 - \Re\left(a(e^{j\omega_c})^2 v^2 e^{j2\omega_c t}\right)\right)$$
$$\beta_t r_t = \frac{1}{2}\left(\Re\left\{w(e^{j\omega_c})\right\}|v|^2 - \Re\{w(e^{j\omega_c})v^2 e^{j2\omega_c t}\}\right)$$
$$r_t^2 = \frac{1}{2}\left(|v|^2 - \Re\{v^2 e^{j2\omega_c t}\}\right). \quad (25)$$

Since (18) is a linear system driven by the two inputs $\beta_t r_t$, and r_t^2, both with two pure sinusoidal components (with frequencies 0 and $2\omega_c$) the output (16) will also be a sum of two sinusoids. Computing the complex amplitudes of these sinusoidal components of $\mathbb{E}[y_t^2]$, and replacing the resulting expression for $\mathbb{E}[y_t^2]$ and (25) in (15), we obtain (20).

It is clear that $b(1) = c(1)$ and $b(-1) = c(-1)$ and thus $\text{var}(y_t) = 0$ when $\omega_c \in \{0, \pi\}$; $b(1) = 0$ follows from:

$$\text{var}(y_t) = b(1)|v|^2 \left(1 - \cos(2\psi_v)\right) \quad (26)$$

obtained by setting $\omega_c = 0$ in (20). For $\psi_v = 0$, i.e., $r_t = |v|$, we conclude that $\text{var}(y_t)$ is identically zero. If we pick $v \neq 0$, $\psi_v' \in (0, \pi/4)$, and $v' = v/\sin(\psi_v')$ and make $r_t = |v'|\sin(\psi_v') = |v|$ then $\text{var}(y_t)$ must also be identically zero, but (26) gives $b(1)|v'|^2(1 - \cos(2\psi_v'))$, which implies $b(1) = 0$.

PROOF OF THEOREM 3

Consider first a periodic r characterized by the Fourier transform (7). We assume that the period T is odd (the proof for an even T follows similar arguments). Then

$$r_t = \frac{1}{T}\sum_{k=0}^{T-1} v_k e^{jw_k t} = \frac{1}{T}\left(v_0 + 2\sum_{k=1}^{\frac{T-1}{2}} \Re\{v_k e^{jw_k t}\}\right) \quad (27)$$

for every $t \in \mathbb{Z}$. Let $y_{k,t}$, $k \in \mathcal{P} := \{1, \ldots, (T-1)/2\}$ and $y_{0,t}$ denote the stochastic processes coinciding with the output response of the closed-loop system to $\Re\{v_k e^{j w_k t}\} = \Im\{v_k j e^{j w_k t}\}$ and v_0, respectively. Then, from Theorem 2, we conclude that for each $k \in \{1, \ldots, (T-1)/2\}$

$$\mathrm{var}(y_{k,t}) = b(e^{j\omega_k})|v_k|^2 + \Re\left(c(e^{j\omega_k})v_k^2 e^{2\omega_k t}\right)$$

and $\mathrm{var}(y_{0,t}) = 0$, for every $t \in \mathbb{Z}$. Moreover, due to the linearity of the system, the response of the closed-loop system to (27) is a stochastic process given by

$$y_t = \frac{1}{T}\left(y_{0,t} + 2\sum_{k=1}^{\frac{T-1}{2}} y_{k,t}\right). \tag{28}$$

We fix $t \in \mathbb{Z}$ and define a one-to-one map $\mu : \mathcal{P} \to \mathcal{P}$ which orders the random variables $y_{k,t}$ by decreasing order of variance, i.e.,

$$\mathrm{var}\left(y_{\mu(\ell+1),t}\right) \leq \mathrm{var}\left(y_{\mu(\ell),t}\right), \quad \ell \in \left\{1, \ldots, \frac{T-1}{2} - 1\right\}. \tag{29}$$

Using the Cauchy-Schwarz inequality, for $\ell \geq \kappa$, $\ell, \kappa \in \mathcal{P}$

$$R_{\ell\kappa} \leq \sqrt{\mathrm{var}\left(y_{\mu(\ell),t}\right)\mathrm{var}\left(y_{\mu(\kappa),t}\right)} \leq \mathrm{var}\left(y_{\mu(\kappa),t}\right) \tag{30}$$

where $R_{\ell\kappa} := \mathbb{E}[(y_{\mu(\ell),t} - \mathbb{E}[y_{\mu(\ell),t}])(y_{\mu(\kappa),t} - \mathbb{E}[y_{\mu(\kappa),t}])]$ (the dependence of $R_{\ell\kappa}$ and μ on t is omitted). Then

$$\mathrm{var}[y_t] = \mathbb{E}\left[\left(\frac{1}{T}\left(y_{0,t} - \mathbb{E}[y_{0,t}] + 2\sum_{\ell=1}^{\frac{T-1}{2}}(y_{\ell,t} - \mathbb{E}[y_{\ell,t}])\right)\right)^2\right]$$

$$= \frac{4}{T^2}\sum_{\ell=1}^{\frac{T-1}{2}}\sum_{\kappa=1}^{\frac{T-1}{2}} R_{\ell\kappa}$$

$$= \frac{4}{T^2}\left(\sum_{\ell=1}^{\frac{T-1}{2}}\left(\mathrm{var}\left(y_{\mu(\ell),t}\right) + 2\sum_{\kappa=\ell+1}^{\frac{T-1}{2}} R_{\mu(\ell)\mu(\kappa)}\right)\right)$$

$$\leq \frac{4}{T^2}\left(\sum_{\ell=1}^{\frac{T-1}{2}}\left(1 + 2\left(\frac{T-1}{2} - \ell\right)\right)\mathrm{var}\left(y_{\mu(\ell),t}\right)\right)$$

$$\tag{31}$$

$$\leq \frac{4}{T}\sum_{\ell=1}^{\frac{T-1}{2}}\mathrm{var}\left(y_{\mu(\ell),t}\right)$$

$$= \frac{4}{T}\sum_{\ell=1}^{\frac{T-1}{2}} b(e^{j\omega_\ell})|v_\ell|^2 + \Re\left(c(e^{j\omega_\ell})v_\ell^2 e^{2\omega_\ell t}\right)$$

$$\leq \frac{4}{T}\sum_{\ell=1}^{\frac{T-1}{2}}\left(\left|b(e^{j\omega_\ell})\right| + \left|c(e^{j\omega_\ell})\right|\right)|v_\ell|^2 \tag{32}$$

which is (22). To establish the second equality, we used the fact that $y_{0,t} = \mathbb{E}[y_{0,t}]$ (since $\mathrm{var}(y_{0,t}) = 0$) for every $t \in \mathbb{Z}$ and to establish (31) we used (30).

Consider now a signal r with bounded energy but also with finite support, i.e., zero outside the interval $t \in \mathcal{M} := \{-m, \ldots, m\}$ for a given $m \in \mathbb{N}$. Let $\tilde{r}_t$ be a periodic signal with odd period $T > 2m$ which equals r_t in the interval $t \in \mathcal{T} := \{-((T-1)/2), \ldots, (T-1)/2\}$. Let $\tilde{\beta}_t$ and $\tilde{\zeta}_t$ denote the solutions to (9) and (18), respectively, when $\tilde{r}_t$ is the input. It follows from the linearity and the stability of (9) that $\max_{t \in \mathcal{M}} |\beta_t - \tilde{\beta}_t| < \epsilon_T$, where $\epsilon_T \to 0$ as $T \to \infty$. Since $\tilde{\zeta}_t$ is obtained by the solution of a linear system (18) with inputs $\tilde{\beta}_t \tilde{r}_t$ and $\tilde{r}_t$ one can also conclude that $\max_{t \in \mathcal{M}} |\zeta_t - \tilde{\zeta}_t| < \tau_T$, where $\tau_T \to 0$ as $T \to \infty$. Then we conclude that the variance of the responses are arbitrarily close as $T \to \infty$. The variance for $\tilde{r}$ can be bounded by (22) which is then also a bound for the variance of the response to r. Moreover since this bound (22) holds for every $T > 2m$ it also holds if we take the limit as $T \to \infty$. Note that $v_k = \hat{r}(e^{j\omega_k})$, $\omega_{k+1} - \omega_k = 2\pi/T$, and then (22) is an approximation to the integral (21). This approximation converges as $T \to \infty$ since the integrand in (21) is bounded and infinitely differentiable. In fact, $\hat{r}(e^{j\omega}) = \sum_{t=-m}^{m} r_t e^{-j\omega t}$ is a sum of bounded and differentiable functions of ω, and $b(z)$ and $c(z)$ are rational functions of $z = e^{j\omega}$, and differentiable and bounded functions of ω since $\mathrm{r}(M) < 1$, $\mathrm{r}(\bar{E}) < 1$ due to Assumption 2.

Consider now a general signal r_t with bounded energy, and make $r_t = z_t + u_t$, $z_t = r_t$ for $t \in \mathcal{M}$, and $z_t = 0$ otherwise, and $u_t = r_t$, for $t \in \mathbb{Z} \setminus \mathcal{M}$, $u_t = 0$ otherwise. By linearity of the system $y_t = y_{u,t} + y_{z,t}$, where $y_{u,t}, y_{z,t}$ are the output responses to u and z, respectively. Since r has bounded energy, $\sum_{t=-\infty}^{\infty} |u_t|^2 < \epsilon_m$ where $\epsilon_m \to 0$ as $m \to \infty$. This implies that $\sum_{t=-\infty}^{\infty} |\mathbb{E}[y_{u,t}]|^2 < \tau_m$ and $\sum_{t=-\infty}^{\infty} |\mathrm{var}[y_{u,t}]| < \pi_m$, where $\tau_m \to 0$, $\pi_m \to 0$ as $m \to \infty$. Then, since

$$\mathrm{var}(y_t) = \mathrm{var}(y_{u,t}) + \mathrm{var}(y_{z,t})$$

$$+ 2\mathbb{E}\left[(y_{z,t} - \mathbb{E}[y_{z,t}])(y_{u,t} - \mathbb{E}[y_{u,t}])\right]$$

$$\leq \mathrm{var}(y_{u,t}) + \mathrm{var}(y_{z,t}) + 2\sqrt{\mathrm{var}(y_{z,t})\mathrm{var}(y_{u,t})}$$

for each $t \in \mathbb{Z}$ we conclude that $\lim_{T \to \infty} \max_{t \in \mathbb{Z}} |\mathrm{var}(y_t) - \mathrm{var}(y_{z,t})| = 0$. Therefore, since (22) is a bound to $\mathrm{var}(y_{z,t})$ for arbitrarily large T it is also a bound to $\mathrm{var}(y_t)$.

Remark 4: Note that (31), (32) provide tighter bounds to the variance than (22), which depend on time $t \in \mathbb{N}$. Similar bounds can be obtained for the case of finite energy inputs.

REFERENCES

[1] B. Lincoln and A. Cervin, "Jitterbug: A tool for analysis of real-time control performance," in *Proc. 41st IEEE Conf. Decision and Control*, Dec. 2002, vol. 2, pp. 1319– 1324.

[2] V. Gupta, A. Dana, J. Hespanha, R. Murray, and B. Hassibi, "Data transmission over networks for estimation and control," *IEEE Trans. Autom. Control*, vol. 54, no. 8, pp. 1807– 1819, Aug. 2009.

[3] L. Schenato, B. Sinopoli, M. Franceschetti, K. Poolla, and S. Sastry, "Foundations of control and estimation over lossy networks," *Proc. IEEE*, vol. 95, no. 1, pp. 163– 187, Jan. 2007.

[4] G. F. Franklin, D. J. Powell, and A. Emami-Naeini, *Feedback Control of Dynamic Systems*, 4th,   Upper Saddle River, NJ: Prentice-Hall, 2001.

[5] O. L. V. Costa, M. Fragoso, and R. P. Marques, *Discrete-Time Markov Jump Linear Systems*,   New York, NY, USA: Springer-Verlag, 2005.

[6] A. V. Oppenheim, A. S. Willsky, and S. H. Nawab, *Signals & Systems*. Upper Saddle River, NJ: Prentice-Hall, 1997.

[7] D. Antunes, W. Geelen, and W. Heemels, " Frequency-domain analysis of real-time and networked control systems with stochastic delays and drops," in *Proc. European Control Conf. (ECC)*, Jul. 2015, pp. 934–940.